

## Surface magnetic properties of ultrathin Fe films on W(110) studied by spin-resolved appearance potential spectroscopy

G. Rangelov, H. D. Kang, J. Reinmuth, and M. Donath

Max-Planck-Institut für Plasmaphysik, EURATOM Association, Surface Physics Division, D-85740 Garching bei München, Germany

(Received 16 July 1999)

The surface sensitivity of spin-resolved appearance potential spectroscopy (APS) was exploited to investigate the magnetic properties of ultrathin Fe layers on W(110). The spin asymmetry, used to monitor the magnetic moment within the probing depth of APS, was studied as a function of the Fe film thickness. The spin asymmetry data reveal a pronounced maximum at a film thickness of  $\approx 6$  monolayers (ML), which is attributed to the complex film morphology in this thickness range. For thicker, structurally relaxed films, APS measurements with variable sampling depth show the Fe surface magnetic moments enhanced compared with the moments of the sublayers. The spin asymmetry data are analyzed within a simple model.

### I. INTRODUCTION

Ultrathin magnetic films and hetero-structures have attracted increasing attention in recent years. The reduced dimensionality leads to a new class of phenomena different from bulk properties and with promising applications in the data storage technology.<sup>1</sup> Experimental techniques for film characterization able to supply magnetic information together with high elemental-chemical, structural, and surface sensitivity are welcome. Such a method is appearance potential spectroscopy (APS). When a solid surface is bombarded with electrons with sufficient energy, ionization of core levels in the surface region takes place. The created core holes recombine via Auger-electron or x-ray emission. Monitoring the Auger-electron or soft x-ray intensity as a function of the electron kinetic energy reveals the ionization thresholds. In the simplest one-electron picture the signal above the excitation threshold is proportional to the self-convolution of the local density of unoccupied states.<sup>2</sup> In a band ferromagnet below the Curie temperature the electronic structure is exchange split and the magnetization is proportional to the difference of the occupation numbers of majority and minority electrons. By using a spin-polarized electron beam for excitation, one obtains element-specific information about the electronic structure of magnetic solids. The magnetic information is contained in the spin asymmetry  $A$ , which equals the normalized intensity difference between the APS signals for primary electrons polarized parallel (minority) or antiparallel (majority) to the sample magnetization. Spin-resolved APS was applied to elemental magnetic materials such as Fe and Ni,<sup>3-5</sup> to ultrathin Fe films on Cu(001),<sup>6,7</sup> and to compound materials like FeNi<sub>3</sub>.<sup>8,9</sup> In this paper we have exploited the surface sensitivity of spin-resolved APS in order to obtain surface specific magnetic information.

We investigated the relatively well-known Fe/W(110) system.<sup>10</sup> Due to the much higher surface energy of W(110), the Fe films grow on W(110) at room temperature (RT) in a layer-by-layer mode.<sup>11,12</sup> Despite of the lattice mismatch of 9.4% between W and Fe, the first 1.8 ML form a pseudomorphic overlayer. During growth of further layers the tensile stress is continuously released by a dislocation network. Finally, at thicker films above 9 ML the Fe bcc lattice constant is adopted.<sup>13</sup> Annealing of room-temperature grown Fe

films thinner than 10 ML at 350–500 K leads to smooth and well-ordered surfaces as shown in the literature by several authors.<sup>14,15</sup> High-quality thicker films are obtained by depositing the Fe layers in excess of 10 ML while increasing the sample temperature to 550 K. Annealing the films above a certain thickness-dependent temperature leads to film disruption. Three-dimensional islands are formed which are surrounded by areas with thin pseudomorphic Fe films covering the W(110) surface.<sup>11,16,15</sup> For Fe films thinner than  $\approx 45 \pm 5$  ML the direction of easy magnetization is along the  $[1\bar{1}0]$  crystallographic axis.<sup>17</sup> Above 50 ML the direction of easy magnetization rotates in the film plane by  $90^\circ$  to  $[001]$ ,<sup>17</sup> which is the easy axis of bulk bcc Fe.

Due to the reduced coordination number of the surface atoms an increase of the surface magnetic moment  $\mu_{\text{surf}}$  is expected. It has been predicted theoretically<sup>18,19</sup> that the surface magnetic moment of Fe films on W(110) is enhanced to  $2.64\mu_B$  with respect to the bulk value of  $2.22\mu_B$ . However, experimental data obtained with spin-polarized low-energy electron diffraction by Waller *et al.*<sup>20</sup> and Tamura *et al.*<sup>21</sup> observed a much higher Fe surface magnetic moment. It varies between  $2.9\mu_B$  and  $3.1\mu_B$ , depending on the model assumptions used to analyze the data.<sup>21,22</sup> More recent magnetometry measurements by Albrecht *et al.*<sup>23,24</sup> obtained  $\mu_{\text{surf}} = (2.7 \pm 0.2)\mu_B$  for the smooth surface in agreement with the theoretical value. The discrepancy between both experimental results might be due either to the different experimental approach and their particular data analysis or to a different film quality in both experiments. The latter possibility is supported by the fact that for step and kink atoms even higher magnetic moments of up to  $3.5\mu_B$  are reported and therefore, the average surface magnetic moment depends on the surface defect concentration.<sup>23,24</sup> APS is well suited to tackle this problem due to its ability to supply surface specific magnetic information as we will demonstrate in this paper.

### II. EXPERIMENT

The experiments were performed in a UHV chamber with a base pressure of  $\approx 3 \times 10^{-11}$  mbar. Besides APS, the ap-

paratus was equipped with low-energy electron diffraction (LEED) and Auger-electron spectroscopy (AES) for surface characterization, a quadrupole mass spectrometer for residual gas analysis, electron beam evaporators for depositing ultra-thin films, and a quartz microbalance for film thickness calibration. The APS experiment consists of a source for spin-polarized electrons<sup>25</sup> and a detector for soft x rays.<sup>26</sup> The electron beam (sample currents typically 40  $\mu\text{A}$ ) is transversally polarized. The polarization is reversed by changing the direction of circular polarization of the laser light used to excite spin-polarized electrons from the GaAs photocathode. Either the sample or the GaAs crystal are biased at high voltage which determines the electron kinetic energy. The soft x-ray photons emitted from the sample pass a filter placed in front of a microchannel plate (MCP) to reduce the low-energy background. A CsI layer of  $\approx 1600$   $\text{\AA}$  thickness, acting as a transmission photocathode, is vacuum evaporated onto the microchannel plate side of an additional 1000  $\text{\AA}$  self-supporting amorphous carbon filter. The electrons emitted from this "photon-to-electron converter" are detected by the MCP. The overall acceptance of the detector is estimated to be  $\Omega \approx 0.2$  sr. In order to suppress further the high background intensity we used a modulation technique with lock-in detection. The electron kinetic energy is modulated with an ac voltage of typically 0.5–4.0 V peak-to-peak and 0.8–1.2 kHz modulation frequency. The APS detector is described in detail in the literature.<sup>26</sup>

The W(110) crystal was prepared by standard cleaning procedures including a prolonged annealing at 1500 K in a  $1 \times 10^{-7}$  mbar oxygen atmosphere and a subsequent flash in UHV to 2500 K. The surface condition of the sample was controlled with AES, APS and LEED. The Fe films were evaporated on the clean W(110) substrate by an electron beam evaporator with a rate of  $\approx 0.5$  ML/min. For the first 6 ML the sample was kept at 300 K during evaporation. To improve the surface order the sample was subsequently annealed at 350 K. For thicker films the sample temperature during evaporation was continuously increased up to 550 K. This preparation procedure results in an almost layer-by-layer growth of well-ordered Fe films with sharp LEED patterns.<sup>14,15</sup> The Fe coverage  $\Theta_{\text{Fe}}$  was determined via characteristic LEED patterns<sup>12</sup> and kinks in the Fe Auger amplitude curve, which indicate the completion of atomic layers,<sup>11</sup> with an estimated accuracy of 10%.

For  $\Theta_{\text{Fe}} > 45 \pm 5$  ML an in-plane rotation of the easy magnetization direction from  $[1\bar{1}0]$  to  $[001]$  takes place.<sup>17</sup> Therefore, special magnetization coils able to magnetize in both directions were used. External fields for magnetization of up to  $\approx 12$  mT were applied.

### III. RESULTS AND DISCUSSION

Figure 1 presents spin-integrated APS spectra for the Fe  $2p$  threshold above 700 eV as a function of the energy for different Fe coverages. All spectra are normalized to equal maximum intensity. With increasing film thickness, several changes are observed: (i) The spectral features shift continuously to higher primary energies  $E_p$ . The maximum shift is  $\approx 0.5$  eV. (ii) The intensity of the  $2p_{3/2}$  component increases relative to the intensity of the  $2p_{1/2}$  component. (iii) Most significantly, a new spectral feature at  $E_p \approx 715$  eV

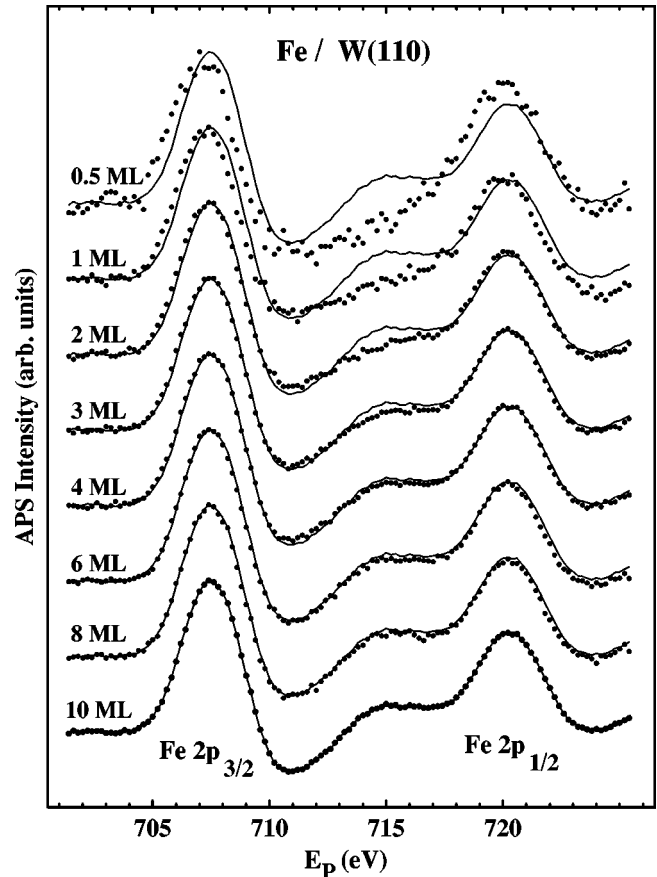


FIG. 1. Spin-integrated APS spectra for Fe films on W(110). For comparison, the data for 10 ML are included as solid lines in the spectra for thinner films.

appears. All changes noted above saturate for  $\Theta_{\text{Fe}}$  between 4 and 6 ML. The APS spectrum of the 10-ML film resembles the spectrum of bulk Fe (Refs. 4,5) indicating a bulklike electronic structure of 10 ML. For reasons of comparison, the 10-ML spectrum is superimposed on all other spectra as a solid line.

In a first approximation the APS spectra represent a self-convolution of the density of unoccupied states. Therefore, the observed energy shift of the  $2p$  spectral features can be due either to a shift of the binding energy of the initial core level or to changes in the unoccupied local density of states.<sup>8</sup> Hong *et al.*<sup>27</sup> calculated the density of states (DOS) of 1 ML Fe/W(110) as well as for bulk Fe. The calculations show a strong hybridization between  $d$  states of Fe and W, which results in a shift of the unoccupied minority states of the Fe monolayer towards the Fermi level. According to our model calculations this leads to a shift of the APS spectrum for 1 ML Fe/W(110) towards lower primary energy with respect to the bulk spectrum.<sup>28</sup> The expected shift of  $\approx 0.8$  eV is much higher than the observed one of  $\approx 0.3$  eV. The difference can be explained by a downward shift of the core-level binding energy of  $\approx 0.5$  eV.

It is well-known that the branching ratio  $B_r = I(2p_{3/2})/[I(2p_{3/2}) + I(2p_{1/2})]$  in the case of x-ray absorption spectroscopy (XAS) depends on the material. In a theoretical study Thole *et al.*<sup>29</sup> attributed this phenomenon to the variation of the occupation number of the valence  $d$  band. In the case of the APS process, the final state contains two

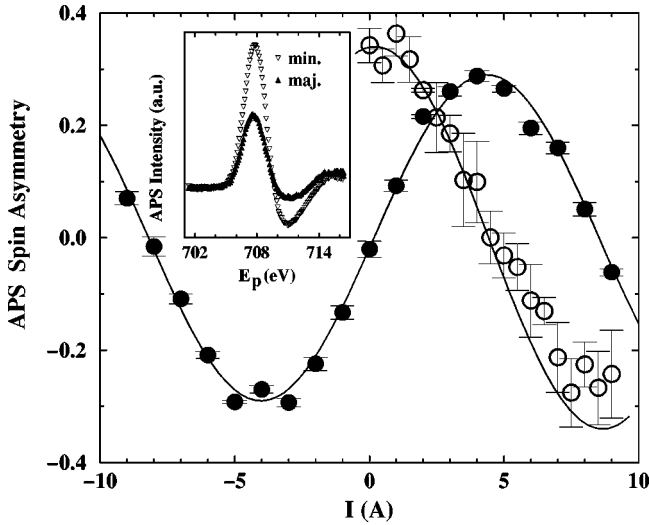


FIG. 2. Fe APS spin asymmetry of the APS signal for Fe  $2p_{3/2}$  as a function of the coil current  $I$  of the spin rotator. Empty dots: 10 ML Fe/W(110). Full dots: 55 ML Fe/W(110). Solid lines: cosine fit. Inset: spin-resolved APS spectra for Fe  $2p_{3/2}$ .

electrons in the valence band and a hole at the initial core level. This excited state relaxes by emission of either an Auger electron or an x-ray photon. In our case we detect photons. Therefore, the deexcitation of the final APS state is the time-reversed process with respect to the XAS excitation. The difference is that there are two electrons in the valence band instead of one as in the case of XAS. Due to the hybridization of Fe and W  $d$  states at the interface, the occupation of the valence  $d$  band for lower coverages is different from that in bulk Fe,<sup>27</sup> which may be responsible for the observed increase of the branching ratio.

The spectral feature at  $E_p \approx 715$  eV is caused by details of the unoccupied Fe DOS. Dose *et al.*<sup>30</sup> showed that this peak is due to a high density of  $sp$ -like states in the vicinity of a high symmetry point of the Brillouin zone. Because of the delocalized nature of the  $sp$  states, the spectral feature is sensitive to the crystalline structure of the film. This explains its absence for low coverages where the three-dimensional bcc structure of Fe is not fully developed.

The use of spin-polarized electrons for APS measurements provides access to the magnetic properties of the sample. An example of spin-resolved APS data for Fe is shown in the inset of Fig. 2. The normalized difference between the APS signals for minority ( $I_\downarrow$ ) and majority ( $I_\uparrow$ ) electrons is defined as the spin asymmetry  $A$ . It is given by the scalar product of the effective magnetic moment  $\tilde{\mu}$ , i.e., the magnetic moment per atom averaged and weighted within the APS information depth, and the electron beam polarization  $\vec{P}$ :

$$A = \frac{I_\downarrow - I_\uparrow}{I_\downarrow + I_\uparrow} = \kappa(\text{DOS}) \tilde{\mu} P \cos\beta, \quad (1)$$

where  $\beta$  is the angle between  $\vec{P}$  and  $\tilde{\mu}$ . The proportionality factor  $\kappa$  accounts for coverage-dependent changes in the spin-resolved DOS which influences the shape of the APS peak and, as a consequence, the asymmetry. Since  $A$  is a function of  $E_p$ , it is important to determine  $A$  in a defined

way. We used two ways to deduce  $A$ . (i) We measured the total  $2p_{3/2}$  APS line, calculated  $A(E_p)$  from the spin-resolved intensities with the spin-independent background subtracted, and integrated over a 1.2 eV energy interval around the peak maximum. (ii) In order to reduce the data acquisition time, we measured  $I_\uparrow$  and  $I_\downarrow$  for two values of  $E_p$  only: at the peak maximum and within the background below threshold. For these two-point measurements we increased the modulation amplitude up to 4 eV in order to integrate over a wider energy interval. The asymmetry values obtained in both ways are comparable when scaled by a factor depending only on the integration interval and the modulation amplitude used.

To maximize the experimental spin asymmetry and to monitor spin reorientation transitions, one needs the option to align the electron spin polarization and the sample magnetization  $\mathbf{M}$ . In our experiment, we included a spin rotator in our electron optics able to rotate the electron spin polarization within the transversal plane. This is achieved by a solenoid coil producing a magnetic field parallel to the direction of propagation of the electron beam and perpendicular to its spin polarization. Figure 2 proves the performance of this spin rotator. The APS spin asymmetry is shown as a function of the coil current for 10 ML (empty dots,  $\mathbf{M} \parallel [1\bar{1}0]$ ) and 55 ML (full dots,  $\mathbf{M} \parallel [001]$ ) of Fe on W(110).  $A$  was determined by the two-point method described above. The 10 ML (55 ML) data reveal a maximum (zero) at zero magnetic field according to the relative orientation of the magnetization and the spin polarization. The APS spin asymmetry increases (decreases) for the 10 ML (55 ML) film with increasing coil current and the situation reverses at  $\approx 4.5$  A, which indicates a rotation of the spin polarization by  $90^\circ$ . For a coil current of about 9 A the spin asymmetry for the 10 ML (55 ML) film reaches a minimum (zero) corresponding to a reversal of the initial spin polarization. By reversing the current direction (shown only for the 55 ML film) a full cycle can be measured. The solid lines are cosine fits to the experimental data. The fits describe the experimental data quite well. The period of the cosine function is  $\approx 18$  A and the phase shift between both cosine functions is  $90^\circ$  as expected from the discussed reorientation transition. A closer inspection of the data shows two additional effects. First, the maximum values for 10 and 55 ML are not equal and the absolute values of the extrema for the 10 ML data also differ considerably. These differences are due to a reduction of the transversal spin polarization after rotation in the magnetic field owing to field inhomogeneities. Based on our data, we estimate a polarization reduction of  $\approx 20\%$  after a rotation of  $180^\circ$ . Therefore, we need to rescale all data obtained with the spin rotator. Second, the APS spin asymmetry for the 55 ML film is slightly negative at zero coil current. This means that the angle between the electron spin polarization and the sample magnetization is not exactly  $90^\circ$ . This is attributed to a slight geometrical misalignment of the sample mounting and to influences of the earth magnetic field. The combined effect of both contributions was estimated to be less than  $3^\circ$ .

Figure 3 shows the APS spin asymmetry as a function of the Fe film thickness at two different sample temperature of 150 (dots) and 300 K (triangles). The asymmetry data were extracted from APS spectra of the full  $2p_{3/2}$  line. The dashed line is just a guide to the eye. For 1 ML no spin asymmetry

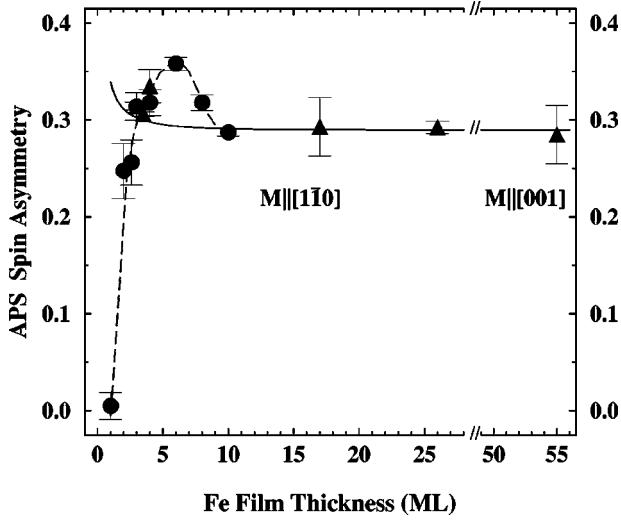


FIG. 3. Spin asymmetry of the Fe  $2p_{3/2}$  APS signal as a function of the Fe film thickness. Different symbols correspond to different experimental series (for details see text).

was detected. With increasing  $\Theta_{\text{Fe}}$  the asymmetry increases rapidly, passes a broad maximum at about 6 ML, and saturates for thicknesses above 10 ML. The asymmetry data for 55 ML are obtained by rotating the spin polarization of the incoming electron beam in the [001] direction. The polarization reduction is taken into account. For 1 ML Fe/W(110) the Curie temperature  $T_C$  is reported to be 210 K.<sup>31,32</sup> For  $\Theta_{\text{Fe}} \geq 2$  ML the Curie temperatures are higher than 450 K (Ref. 32) approaching the bulk Curie temperature of Fe at 1043 K for higher coverages. As a consequence, the sample temperature was well below  $T_C$  of the film and therefore the lower asymmetry values at  $\Theta_{\text{Fe}} \leq 2.5$  ML cannot be explained by a low  $T/T_C$ . Most probably our magnetic field was not high enough to completely magnetize the film. Indeed, Sander *et al.*<sup>33,34</sup> observed high in-plane coercivity in this thickness range.

How can we explain the asymmetry maximum, which suggests, according to Eq. (1), a coverage dependence of the effective magnetic moment? Provided the sample temperature is well below  $T_C$  and the magnetic moment per atom is independent of the coverage we expect a constant value of  $A$  as a function of the film thickness, which is the case for films thicker than 10 ML. Obviously, we need either a pronounced change of the DOS or an enhanced effective magnetic moment in order to understand the asymmetry maximum [compare with Eq. (1)]. As we mentioned above the surface magnetic moments are enhanced by  $\sim 23\%$  at least and even higher values are possible for step atoms.<sup>23,24</sup>

In order to explain the observed asymmetry maximum we calculated the APS asymmetry using a simple model. We simulate the APS signal of  $n$  Fe layers,  $I_{\uparrow,\downarrow}^n$ , as a sum of a surface contribution  $I_{\uparrow,\downarrow}^s$  and, with the assumption that all deeper layers are identical, a contribution of the remaining  $(n-1)$  layers  $I_{\uparrow,\downarrow}^{n-1}$ :

$$I_{\uparrow,\downarrow}^n = I_{\uparrow,\downarrow}^s + I_{\uparrow,\downarrow}^{n-1}. \quad (2)$$

$I_{\uparrow,\downarrow}^{n-1}$  is a sum of contributions from the  $(n-1)$  layers weighted with the sampling depth  $\lambda \cos\theta$ . It is worth noting

that, for the inelastic mean free path, we did not use the value from the universal curve ( $\approx 6$  ML) as usually done by many authors, but the Fe-specific value, namely,  $\lambda = 3.8$  ML for  $E_p = 707$  eV.<sup>35</sup>  $\theta$  denotes the angle of incidence of the incoming electron beam with respect to the surface normal.

$$I_{\uparrow,\downarrow}^{n-1} = \sum_{k=1}^{n-1} I_{\uparrow,\downarrow}^b \exp[-k/(\lambda \cos\theta)], \quad (3)$$

where  $I_{\uparrow,\downarrow}^b$  is the unattenuated contribution from a single bulk layer and  $k$  is the layer number. Then, the asymmetry  $A_n$  of  $n$  Fe layers is

$$A_n = \frac{I_{\downarrow}^n - I_{\uparrow}^n}{I_{\downarrow}^n + I_{\uparrow}^n}. \quad (4)$$

Using Eq. (2) and assuming enhanced asymmetry from the surface layer

$$I_{\downarrow}^s - I_{\uparrow}^s = \alpha(I_{\downarrow}^b - I_{\uparrow}^b) \quad (5)$$

but identical spin integrated APS signals which is supported by Fig. 1

$$I_{\downarrow}^s + I_{\uparrow}^s = I_{\downarrow}^b + I_{\uparrow}^b \quad (6)$$

one obtains

$$A_n = \frac{\alpha - 1}{1 + \sum_{k=1}^{n-1} \exp(-k/\lambda)} A_b + A_b, \quad (7)$$

where

$$A_b = \frac{I_{\downarrow}^b - I_{\uparrow}^b}{I_{\downarrow}^b + I_{\uparrow}^b} \quad (8)$$

is a constant factor representing the asymmetry of a single bulk layer.

With  $\alpha = 1.23$  to account for the theoretically predicted enhancement of the surface magnetic moment,<sup>18</sup> a fit to the saturation value beyond 10 ML gives the solid line in Fig. 3. Note that the model calculations above assume a coverage-independent factor  $\kappa$  [see Eq. (1)]. Indeed, we do not observe changes in the APS line shape (see Fig. 1) as a function of  $\Theta_{\text{Fe}}$ . However, we know from theoretical calculations<sup>27</sup> that the spin-resolved DOS changes as a function of Fe coverage. Obviously, APS is not sensitive to small changes in the layer-dependent DOS. This does not come as a surprise because the APS signal is a derivative of the self-convolution of the unoccupied DOS weighted by the inelastic mean free path. Our model explains a decrease of  $A$  for higher coverages but no maximum. The asymmetry decrease starts at lower coverages and the calculated initial value is lower than the experimental maximum. How can we explain the observed behavior? At this point, one should take into account the structural changes taking place at low coverages.<sup>11,36</sup> The first 1.8 ML of Fe grow pseudomorphically on the W(110) surface despite a large lattice misfit of 9.4%. With increasing Fe coverage this misfit is continuously reduced by a periodical network of dislocations observed as a superstructure in LEED (Ref. 11) and directly detected by STM

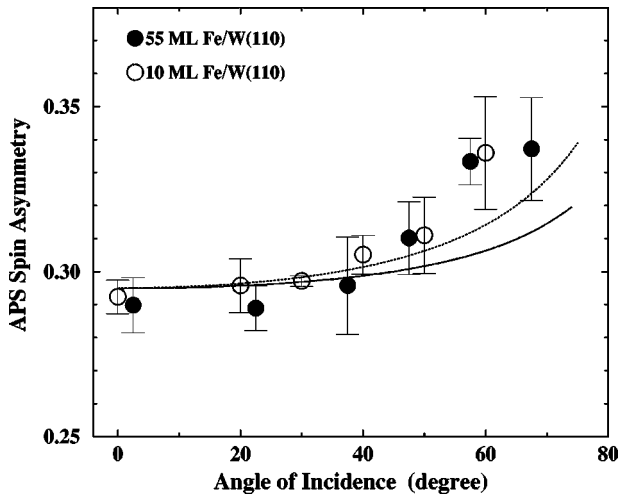


FIG. 4. APS spin asymmetry as a function of the angle of incidence. Empty (full) dots correspond to 10 (55) ML Fe/W(110). The solid (dotted) line represents the model calculation using the theoretical (experimental) values for the Fe surface magnetic moment (for details see text).

measurements.<sup>36</sup> The dislocation network leads to a continuous change of the lattice constant of the film as a function of  $\Theta_{\text{Fe}}$  and to an enhanced corrugation at the surface. These structural changes cause changes in the electronic structure and may lead to enhanced magnetic moments of the Fe atoms. In addition, the growth mode is a statistical layer-by-layer mode<sup>36</sup> which means that at least three layers are exposed, i.e., the number of step and kink atoms is enhanced as well. The enhanced defect density at the surface should enhance the effective surface magnetic moment. For  $\Theta_{\text{Fe}} > 9$  ML the Fe grows in its bulk bcc structure, the strain and the dislocation-induced LEED pattern disappear and the film grows atomically smooth.<sup>11,37</sup> Obviously, our model reproduces only the regime of bcc growth. For the constant bulk contribution we get  $A_b = 0.28$ , which is slightly lower than the saturation asymmetry of 0.29.

To investigate the enhancement of the surface magnetic moment one can enhance the surface sensitivity of APS by increasing the angle of incidence of the incoming electrons [see Eq. (3)]. The results of such an experiment for well-ordered and smooth bcc Fe films are demonstrated in Fig. 4. The angle of electron incidence was varied by rotating the sample around the [001] direction. For these measurements the APS asymmetry was obtained by the two-point method as describe above. The empty and full dots in Fig. 4 represent the results for 10 and 55 ML Fe/W(110), respectively. The sample magnetization is along the  $[1\bar{1}0]$  direction for the 10 ML film and along then [001] direction for the 55 ML film. In the first case a cosine correction according to Eq. (1)

was made. In the latter case the electron polarization is parallel to the sample magnetization for all angles of incidence and no cosine correction is needed. The points for 10 ML and 55 ML show identical angular dependencies. The asymmetry increases with increasing angle of incidence, i.e., with increasing surface sensitivity. This proves clearly the existence of enhanced surface magnetic moments at Fe(110). The asymmetry reaches values as high as 0.34 which is close to the maximum value in Fig. 3.

In order to extract quantitative information about the surface magnetic moments of Fe we calculated the angular dependence of the asymmetry with the simple model discussed above. We assumed the same inelastic mean free path of 3.8 ML, the same enhancement of the surface magnetic moment of 23%, and the same value for  $A_b$  as obtained above. The result is shown in Fig. 4 as a solid line. Obviously, the calculated curve explains qualitatively the experimental data. The agreement can be improved if one increases the assumed surface magnetic moment in the calculation. The dashed line is calculated with a 40% enhancement of the surface magnetic moments. A further increase would improve even more the agreement. Our results are not unexpected in light of measurements of Albrecht *et al.*,<sup>23,24</sup> who estimated a 60% enhancement of the magnetic moments of step Fe atoms. We can not exclude, however, that slight changes in the DOS may also influence the asymmetry, although we have not observed any changes in the APS line shapes as a function of the angle of electron incidence.

#### IV. CONCLUSIONS

We used spin-resolved APS for surface magnetometry on Fe/W(110) based on measurements of the Fe  $2p$  signal. We detected coverage-dependent changes of the APS asymmetry which reflect the structural and electronic (and respectively magnetic) changes taking place during the transition from strained to relaxed bcc iron with increasing Fe film thickness. For thick bulklike bcc Fe films we observed an enhanced spin asymmetry at the surface by varying the information depth of APS. We discussed the results within a simple model. From our spin-resolved APS measurements, we have strong evidence of enhanced magnetic moments both in ultrathin films and at the surface of thicker films of Fe on W(110). Our results confirm the assumption that the APS spin asymmetry is proportional to the effective magnetic moment within the probing depth of the spectroscopy. We showed that quantitative measurements of the surface magnetic properties are possible by spin-resolved APS.

#### ACKNOWLEDGMENTS

We thank V. Dose for helpful discussions. Financial support by the Deutsche Forschungsgemeinschaft is gratefully acknowledged.

<sup>1</sup>U. Gradmann, in *Handbook of Magnetic Materials*, edited by K. H. J. Buschow (Elsevier, Amsterdam, 1993), Vol. 7, Chap. 1, p. 1.

<sup>2</sup>R. Park and J. E. Houston, *J. Vac. Sci. Technol.* **11**, 1 (1974).

<sup>3</sup>J. Kirschner, *Solid State Commun.* **49**, 39 (1984).

<sup>4</sup>M. Vonbank, Ph.D. thesis, Technische Universität Wien, 1992.

<sup>5</sup>K. Ertl, M. Vonbank, V. Dose, and J. Noffke, *Solid State Commun.* **88**, 557 (1993).

<sup>6</sup>Th. Detzel, M. Vonbank, M. Donath, and V. Dose, *J. Magn. Mater.* **147**, L1 (1995).

- <sup>7</sup>Th. Detzel, M. Vonbank, M. Donath, N. Memmel, and V. Dose, *J. Magn. Magn. Mater.* **152**, 287 (1996).
- <sup>8</sup>J. Reinmuth, F. Passek, V. N. Petrov, M. Donath, V. Popescu, and H. Ebert, *Phys. Rev. B* **56**, 12 893 (1997).
- <sup>9</sup>J. Reinmuth, M. Donath, F. Passek, and V. N. Petrov, *J. Phys.: Condens. Matter* **10**, 4027 (1998).
- <sup>10</sup>G. A. Mulhollan, A. B. Andrews, and J. L. Erskine, *Phys. Rev. B* **46**, 11 212 (1992); Di-Jing Huang, D. M. Riffe, and J. L. Erskine, *ibid.* **51**, 15 170 (1995), and references therein.
- <sup>11</sup>U. Gradmann and G. Waller, *Surf. Sci.* **116**, 539 (1982).
- <sup>12</sup>T. M. Gardiner, *Thin Solid Films* **105**, 213 (1983).
- <sup>13</sup>H. Bethge, D. Heuer, Ch. Jensen, K. Reshöft, and U. Köhler, *Surf. Sci.* **331-333**, 878 (1995).
- <sup>14</sup>H. J. Elmers and U. Gradmann, *Appl. Phys. A: Solids Surf.* **A51**, 255 (1990).
- <sup>15</sup>F. Passek, M. Donath, and K. Ertl, *J. Magn. Magn. Mater.* **159**, 103 (1996).
- <sup>16</sup>M. S. Tikhov and E. Bauer, *Surf. Sci.* **232**, 73 (1990).
- <sup>17</sup>U. Gradmann, J. Korecki, and G. Waller, *Appl. Phys. A: Solids Surf.* **A39**, 101 (1986).
- <sup>18</sup>R. H. Victora and L. M. Falicov, *Phys. Rev. B* **31**, 7335 (1985).
- <sup>19</sup>S. Ohnishi, M. Weinert, and A. J. Freemann, *Phys. Rev. B* **30**, 36 (1984).
- <sup>20</sup>G. Waller and U. Gradmann, *Phys. Rev. B* **11**, 6330 (1982).
- <sup>21</sup>E. Tamura, R. Feder, G. Waller, and U. Gradmann, *Phys. Status Solidi B* **157**, 627 (1990).
- <sup>22</sup>A. Ormeci, B. M. Hall, and D. L. Mills, *Phys. Rev. B* **42**, 4524 (1990).
- <sup>23</sup>M. Albrecht, T. Furubayashi, U. Gradmann, and W. A. Harrison, *J. Magn. Magn. Mater.* **104-107**, 1699 (1992).
- <sup>24</sup>M. Albrecht, U. Gradmann, T. Furubayashi, and W. A. Harrison, *Europhys. Lett.* **20**, 65 (1992).
- <sup>25</sup>U. Kolac, M. Donath, K. Ertl, H. Liebl, and V. Dose, *Rev. Sci. Instrum.* **59**, 1933 (1988).
- <sup>26</sup>G. Rangelov, K. Ertl, F. Passek, M. Vonbank, S. Bassen, J. Reinmuth, M. Donath, and V. Dose, *J. Vac. Sci. Technol. A* **16**, 2738 (1998).
- <sup>27</sup>S. C. Hong, A. J. Freeman, and C. L. Fu, *Phys. Rev. B* **38**, 12 156 (1988).
- <sup>28</sup>J. Reinmuth, Ph.D. thesis, Universität Bayreuth, 1998.
- <sup>29</sup>B. T. Thole and G. van der Laan, *Phys. Rev. B* **38**, 3158 (1988).
- <sup>30</sup>V. Dose, A. Härtl, J. Rogozik, and H. Warlimont, *Solid State Commun.* **49**, 509 (1984).
- <sup>31</sup>H. J. Elmers, J. Hauschild, H. Höche, U. Gradmann, H. Bethge, D. Heuer, and U. Köhler, *Phys. Rev. Lett.* **73**, 898 (1994).
- <sup>32</sup>H. J. Elmers, J. Hauschild, H. Fritzsche, U. Gradmann, and U. Köhler, *Phys. Rev. Lett.* **75**, 2031 (1995).
- <sup>33</sup>D. Sander, R. Skomski, C. Schmidhals, A. Enders, and J. Kirschner, *Phys. Rev. Lett.* **77**, 2566 (1996).
- <sup>34</sup>R. Skomski, D. Sander, A. Enders, and J. Kirschner, *IEEE Trans. Magn.* **32**, 4567 (1996).
- <sup>35</sup>M. P. Seah and W. A. Dench, *Surf. Interface Anal.* **1**, 2 (1979).
- <sup>36</sup>C. Jensen, K. Reshöft, and U. Köhler, *Appl. Phys. A: Mater. Sci. Process.* **62**, 217 (1996).
- <sup>37</sup>U. Gradmann, M. Przybylski, H. J. Elmers, and G. Liu, *Appl. Phys. A: Solids Surf.* **A49**, 563 (1989).